

code was used to analyze the theoretical model. To verify the theory, an experimental array was built and tested. Good agreement between the theory and experiment was demonstrated. Based on the experimental data there is no evidence of a blind spot for this phased-array radiator. The assumption that the balun feed can be ignored in the theoretical model was confirmed. Such an assumption is valid only when a blind spot associated with the balun is not present.

#### REFERENCES

- [1] R. J. Mailloux, "Phased array theory and technology," *Proc. IEEE*, vol. 70, no. 3, pp. 246-291, Mar. 1982.
- [2] E. D. Mayer and A. Hessel, "Feed region modes in dipole phased arrays," *IEEE Trans. Antennas Propagat.*, vol. AP-30, no. 1, pp. 66-75, Jan. 1982.
- [3] L. Stark, "Comparison of array element types," in *Phased Array Antennas (Proc. 1970 Phased Array Antenna Symp.)*, A. A. Oliner and G. H. Knittel, Eds. Dedham, MA: Artech House, 1972, pp. 51-66.
- [4] E. Brookner, *Radar Technology*. Dedham, MA: Artech House, 1977, pp. 289-301.
- [5] H. K. Schuman, D. R. Pflug, and L. D. Thompson, "Infinite planar arrays of arbitrarily bent thin wire radiators," *IEEE Trans. Antennas Propag.*, vol. AP-32, no. 4, pp. 364-377, Apr. 1984.
- [6] J. H. Richmond, "Radiation and scattering by thin-wire structures in a homogeneous conducting medium, computer program description," *IEEE Trans. Antennas Propagat.*, vol. AP-22, no. 2, p. 365, Mar. 1974.
- [7] E. Hallen, *Electromagnetic Theory*. New York: Wiley, 1962, p. 62.
- [8] G. A. Thiele and T. H. Newhouse, "A hybrid technique for combining moment methods with the geometrical theory of diffraction," *IEEE Trans. Antennas Propagat.*, vol. AP-23, no. 1, pp. 62-69, Jan. 1975.

### A Template for Shaped-Beam Satellite Antenna Patterns

K. SUDHAKAR RAO, MEMBER, IEEE

**Abstract**—A modified template is proposed for shaped-beam satellite antenna patterns for use in orbit-planning studies of fixed satellite service. Based upon a previously discussed simple model, the template now includes the effects of beam scanning, aperture blockage, and surface errors. It is found to agree well with the measured data on current satellites and is a reasonable upper bound specification for future satellite antennas.

#### I. INTRODUCTION

Shaped-beam satellite antenna patterns have been modeled recently [1] in a template form. However, only the primary parameters (antenna size and peak sidelobe level) have been taken into account in the previous model. The purpose of this communication is to include the secondary effects due to beam scanning, aperture blockage, and surface errors in the earlier model [1] and present a new template for describing the shaped-beam radiation patterns. Simple expressions are developed to incorporate the primary as well as the secondary parameters in the template definitions. Variables of the template are

Manuscript received July 16, 1987; revised December 3, 1987. This work was supported in part by the Canadian Department of Communications under Contract 36100-6-4523/01-ST.

The author is with Spar Aerospace Limited, Satellite and Aerospace Systems Division, 21025 Trans-Canada Highway, Ste. Anne de Bellevue, PQ, Canada H9X 3R2.

IEEE Log Number 8823418.

the coverage area width  $\psi_0$  and the shaping factor  $S$ . The template is compared with measured satellite data on various programs and is found to be in reasonably good agreement.

#### II. DEVELOPMENT OF THE TEMPLATE

The expressions for various angular parameters of the secondary pattern are given earlier [1, eqs. (3)–(6)] in terms of antenna size ( $D/\lambda$ ) and peak sidelobe level ( $S_L$ ) and are utilized here. The gain in the main lobe skirt region outside the coverage area is fitted through a Gaussian curve

$$G(\Delta\theta) = A \cdot \exp \left[ -B \left( 1 + \frac{\Delta\theta}{\theta_b} \right)^2 \right] \quad (1)$$

where  $\Delta\theta$  is the angle from the edge of coverage region and  $\theta_b$  is the 3-dB half-beamwidth ( $\theta_b = 0.5\theta_0$ ) of the elementary beam. The values of the constants  $A$  and  $B$  depend on the position of truncation level of the main lobe skirt function. Since the beam broadening due to secondary effects is considered separately, the main beam truncation angle could be closer to the coverage region than the one given earlier [1]. Based on extensive comparison with measured satellite data [2], the main beam is truncated at an angle corresponding to one fourth of the angular distance between the first sidelobe peak ( $\theta_s$ ) and the first null ( $\theta_n$ ) from  $\theta_n$ . The angular width of the main lobe skirt region is hence given as

$$\Delta\theta_L = (-2.253 - 2.575 S_L)\lambda/D. \quad (2)$$

The constants  $A$  and  $B$  in (1) are calculated from the above equations and using  $G(0) = 0.5$  as

$$B = \ln(0.5/10^{0.1 S_L}) / \{[(14.307 - 3.35 S_L)/(16.56 - 0.775 S_L)]^2 - 1\} \quad (3)$$

and

$$A = 0.5 \exp(B). \quad (4)$$

In general,  $\Delta\theta_L$  and ( $D/\lambda$ ) can be related through

$$\Delta\theta_L = C \cdot \lambda/D. \quad (5)$$

The value of the constant  $C$  for a 27-dB isolation between adjacent coverage areas (or  $S_L = -30$  dB) is given by DiFonzo [3] as 100. However, for shaped beams the gain outside the coverage area falls at a steeper rate (as could be seen later from the measured data in Figs. 2 and 3). From (2), the value of  $C$  is 75 with  $S_L = -30$ . It is typically in the range 75–90 depending on the extent of scanning.

The secondary parameters having significant effect on the satellite antenna radiation outside the coverage area are identified as aperture blockage, surface errors, and beam scanning due to off-focus location of feeds. The common impact of the aforementioned secondary effects on the satellite radiation are main beam broadening due to gain loss and deterioration of sidelobe levels. Simple formulas are derived for the antenna parameters to take into account the secondary effects and are given separately in the Appendix. Satellite antenna radiation outside the coverage regions can now be expressed in terms of three primary parameters ( $\theta_0$  or  $D/\lambda$ ,  $S_L$ , and  $\psi_0$ ) and three secondary parameters ( $s$ ,  $\Delta$ , and  $\delta$ ).  $\psi_0$  is the width of the coverage region ( $\psi_0 = 2\psi_b$ ) in the direction of interest, and the method of obtaining  $\psi_0$  for a given coverage area is explained at the end of this section. Replacing the beamlet angle  $\theta$  with the coverage angle  $\psi$  and using the relation  $\psi = \theta + \psi_b - \theta_b$  and (1), the gain in the main lobe skirt region (in dB)

TABLE I  
PARAMETERS OF THE NEW TEMPLATE FOR DIFFERENT SIDELobe LEVELS

$S_L$ (dB)	$\theta_0$ (degrees)	$\Delta\psi_L$ (degrees)	$A$	$B$	$U$	$V$	$W$	$Z$
-20	64.12 $\lambda/D$	49.25 $\lambda/D$	1.0274	0.7202	0.117	3.1278	0.7680	1.9663
-22	67.22 $\lambda/D$	54.40 $\lambda/D$	1.0549	0.7466	0.232	3.2424	0.8092	1.9484
-24	70.32 $\lambda/D$	59.55 $\lambda/D$	1.0827	0.7726	0.345	3.3553	0.8468	1.9320
-26	73.42 $\lambda/D$	64.70 $\lambda/D$	1.1109	0.7983	0.457	3.4669	0.8812	1.9171
-28	76.52 $\lambda/D$	69.85 $\lambda/D$	1.1397	0.8239	0.568	3.5781	0.9128	1.9033
-30	79.62 $\lambda/D$	75.00 $\lambda/D$	1.1691	0.8494	0.679	3.6889	0.9419	1.8906
-32	82.72 $\lambda/D$	80.15 $\lambda/D$	1.1992	0.8748	0.789	3.7792	0.9689	1.8789
-34	85.82 $\lambda/D$	85.30 $\lambda/D$	1.2300	0.9002	0.899	3.9095	0.9939	1.8680
-36	88.92 $\lambda/D$	90.45 $\lambda/D$	1.2616	0.9255	1.009	4.0194	1.0172	1.8578
-38	92.02 $\lambda/D$	95.60 $\lambda/D$	1.2940	0.9509	1.119	4.1297	1.0389	1.8484
-40	95.12 $\lambda/D$	100.75 $\lambda/D$	1.3273	0.9763	1.230	4.2400	1.0592	1.8396

can be expressed as

$$G_{dB}(\psi) = U - 4V(\psi/\theta_0)^2 \left[ \frac{\psi}{\psi_0} - 0.5 \left( 1 - \frac{\theta_0}{\psi_0} \right) \right]^2, \quad (6)$$

in the region  $0.5 \leq (\psi/\psi_0) \leq 0.5 + W(\theta_0/\psi_0)$

where  $U = 10 \log A$ ,  $V = 4.3429B$ , and

$$W = (-2.253 - 2.575 S_L) / (33.12 - 1.55 S_L).$$

The gain is kept at a constant level corresponding to the peak sidelobe radiation in the region covering  $\psi_L$  ( $\psi_L = W \cdot \theta_0 + \psi_b$ ) and the position of the second sidelobe peak  $\psi_{s2}$ . Therefore, the gain in the near-in sidelobe region is given by

$$G_{dB}(\psi) = S_L; \quad \text{in the region } 0.5 + W(\theta_0/\psi_0) \leq (\psi/\psi_0) \leq 0.5 + Z(\theta_0/\psi_0). \quad (7)$$

The far-out sidelobe region gain slope is taken as  $-20 \log (\psi/\psi_0)$  as used in BSS 1983 fast roll-off patterns and in the earlier template [1]. By equating the gain value at  $\psi = \psi_{s2}$  to  $S_L$ , the gain in the far-out sidelobe region can be expressed as

$$G_{dB}(\psi) = S_L + 20 \log [Z(\theta_0/\psi_0) + 0.5] - 20 \log (\psi/\psi_0), \quad (8)$$

in the region  $\{Z(\theta_0/\psi_0) + 0.5\} \leq \psi/\psi_0 \leq 90/\psi_0$ .

The upper bound of  $(\psi/\psi_0)$  in (8) is taken as  $(90/\psi_0)$  with  $\psi_0$  expressed in degrees. Beyond this region the antenna gain is very much dependent on the spacecraft structure and the location of the antenna with respect to the spacecraft. Various constants describing the template in (6)–(8) are shown in Table I for different values of the peak sidelobe level  $S_L$ . Only the primary parameters ( $\theta_0$ ,  $\psi_0$ , and  $S_L$ ) are considered in the above equations. Defining the beam-broadening factor due to secondary effects as

$$Q = \theta_0(s, \Delta, \delta) / \theta_0 \quad (9)$$

the parameter  $\theta_0$  in (6)–(8) can now be replaced with  $Q \cdot \theta_0$  to account for the secondary effects. The beam broadening factor  $Q$  can be calculated for practical antennas using (12) in the Appendix. Also the variable  $S_L$  should include the secondary effects as shown by (13) in the Appendix. From (6)–(8) it could be seen that the template gain depends on the ratio  $(\theta_0/\psi_0)$ . It is convenient to incorporate the secondary parameters in the template by introducing a new variable  $S$ , called the shaping factor, given by

$$S = Q \cdot \theta_0 / \psi_0. \quad (10)$$

Using (10) in (6)–(8) and expressing the gain as a function of  $\Delta\psi$

(angle from the coverage area edge,  $\Delta\psi = \psi - \psi_b$ ), the new template is given as

$$G_{dB}(\psi) = U - 4V \frac{1}{S^2} \left( \frac{\Delta\psi}{\psi_0} + 0.5S \right)^2, \quad (11a)$$

$$0 \leq \frac{\Delta\psi}{\psi_0} \leq W \cdot S, \quad \text{main lobe skirt region}$$

$$= S_L; \quad W \cdot S \leq \frac{\Delta\psi}{\psi_0} \leq Z \cdot S, \quad \text{near-in sidelobe region} \quad (11b)$$

$$= S_L + 20 \log (Z \cdot S + 0.5) - 20 \log \left( \frac{\Delta\psi}{\psi_0} + 0.5 \right), \quad (11c)$$

$$Z \cdot S \leq \frac{\Delta\psi}{\psi_0} \leq \frac{90}{\psi_0} - 0.5, \quad \text{far-out sidelobe region.}$$

The shaping factor  $S$  in (11) depends on five parameters, namely  $\theta_0$ ,  $\psi_0$ ,  $s$ ,  $\Delta$ , and  $\delta$ . If the secondary effects are negligible, then  $Q = 1$  and  $S$  becomes the ratio  $(\theta_0/\psi_0)$ . For pencil beams with on-focus feeds, the shaping factor becomes unity.  $S$  is less than one for shaped-beam antennas.

A design study is carried out to estimate feasible sidelobe improvements that can be attained in practice taking into consideration both spacecraft and launch vehicle constraints. A C-band antenna is chosen because of the fact that it would be more difficult to suppress the sidelobes for C-band than for Ku-band for a given angular distance from boresight. An existing Brasilsat antenna design is taken as the baseline case for which the sidelobe levels achieved (without any sidelobe specification) were of the order  $-23$  dB relative to peak. The antenna boresight is inside the coverage area (see [1, Fig. 5]) and maximum amount of scanning is one beamwidth. The objective was to suppress the sidelobe levels while maintaining the coverage gain requirements. Design techniques that were employed to achieve this objective include use of additional nulling horns (these horns have very little power and are effective to suppress the sidelobes locally), extra shared horns, larger reflector size, and combinations of all three. These design modifications were optimized and evaluated through computer simulations using standard Spar antenna design software for offset reflector antennas with multiple feeds.

Based on the design study, the sidelobe levels of Brasilsat antenna could be improved to better than  $-30$  dB (relative to peak) by using extra shared horns and using large antenna aperture. Such an improvement is achieved over 15-percent bandwidth and requires a 22-percent increase in the antenna size and a 43-percent increase in

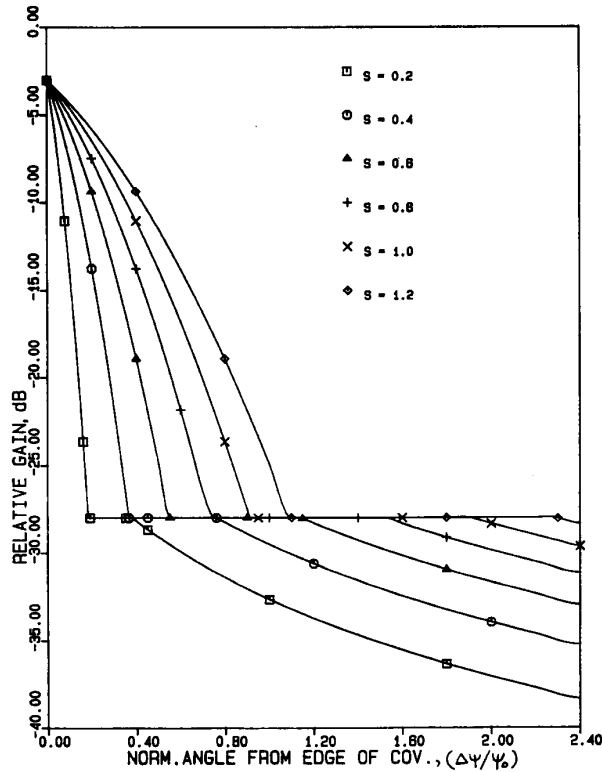


Fig. 1. Recommended template for shaped-beam satellite antennas with peak sidelobe level  $S_L = -28$  dB. Parameter of curves is shaping factor  $S (S = Q\theta_0/\psi_0, Q$  is beam broadening factor due to secondary effects).

the antenna weight (which includes thermal blanket, feed array, supporting structure, etc., weight increases). Details of the results achieved for various design modifications are given in [2]. An implementation margin of at least 2 dB for the peak sidelobe level is necessary from the computed values to realize for practical systems. A peak sidelobe level of 28 dB below peak gain is recommended for future shaped-beam satellite antennas based on the results of the design study. Such a recommendation is made after ensuring that the main beam fall-off rate of the template (with  $S_L = -28$ ) forms a reasonable upper bound envelope for the measured data on Anik-C, G-Star, TDRSS, Brasilsat, and Anik-E (developmental antenna) satellite antennas. The recommended template for future shaped-beam satellites is given by (11) with  $U = 0.568, V = 3.5781, W = 0.9128,$  and  $Z = 1.9033$ .

Normalized template curves are shown in Fig. 1 by plotting the gain as a function of the normalized angle ( $\Delta\psi/\psi_0$ ). The parameter of the curves is the shaping factor  $S$  which is less than one for shaped beams. The curve  $S = 1$  is for pencil beam antennas ( $\theta_0 = \psi_0$ ) with no beam broadening ( $Q = 1$ ), and the curve  $S = 1.2$  is for the pencil beam case with 20-percent main beam broadening. As the value of shaping factor reduces, the main beam gain falls at a steeper rate. For a given coverage region width ( $\psi_0$ ),  $S$  becomes smaller when the beamlet size ( $\theta_0$ ) shrinks which occurs when larger reflector ( $D/\lambda$ ) is used. Also, the width of the constant sidelobe region becomes narrower for highly shaped beams, with smaller value of  $S$ . This aspect has not been considered in the reference patterns proposed in the past [4], [5].

A new hybrid approach is proposed to represent the coverage area unambiguously. In this approach, a minimum area ellipse circumscribing the geographic coverage is used to define the center of coverage area. It is obtained as the intersection of major and minor

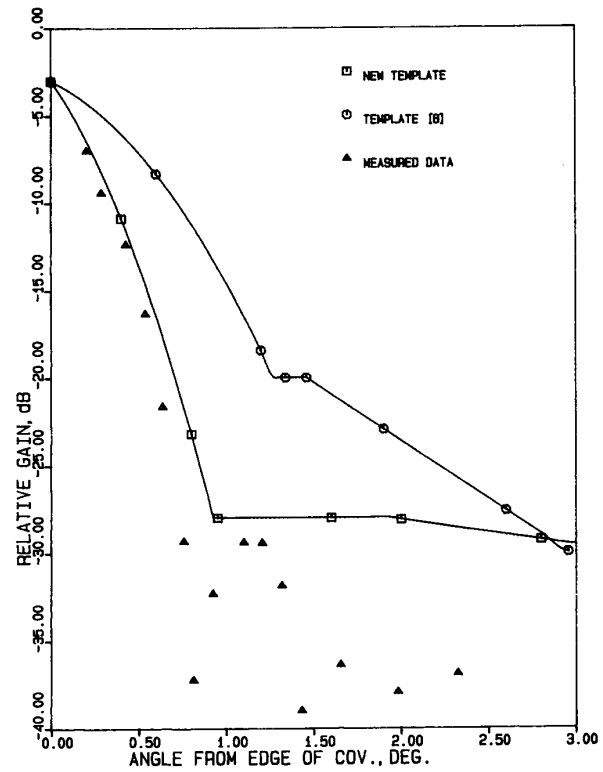


Fig. 2. Comparison of new template with measured data on Anik-E Ku-band developmental antenna (national beam VP-transmit) with  $D/\lambda = 82.96$ . Parameters of template are  $S = 0.145$  and  $\psi_0 = 7.0^\circ$ .

axes of the minimum area ellipse. The center of coverage area does not necessarily represent the beam center and is used only to define the axis of the pattern cuts. A convex polygon is then used to define the coverage area boundary. This is to eliminate ambiguity associated with the concave portions of the coverage area. The number of sides forming the polygon can be determined based on the criteria that it should circumscribe the coverage area as closely as possible and should be of convex shape. An example is shown earlier [1, fig. 1] for the service area representation. The coverage area width  $\psi_0$  is defined as twice the angular distance from the center of coverage to the point of intersection on the convex polygon in the direction of interest. The angular directions should be radial from the center of coverage area.

### III. COMPARISON WITH MEASURED DATA

The recommended template is compared with measured satellite data in this section. Fig. 2 compares the template with measured data on Anik-E developmental antenna designed at Ku-band frequency for the Canadian coverage. Measured data are shown for the National transmit beam with vertical polarization. The antenna size is  $82.96 \lambda$ , and the variables of the template are  $S = 0.145$  and  $\psi_0 = 7^\circ$ . A peak sidelobe level of  $-29$  dB relative to beam maximum has been measured. The template is close to the measurements and forms a reasonable upper bound specification. Also shown in Fig. 2 is the reference pattern proposed recently by the IWP 4/1 [6], [7] which is conservative in the main lobe as well as the sidelobe regions when compared to the measurements and the new template. The template is compared in Fig. 3 with measured data on Brasilsat shaped beam antenna (C-band) in the elevation plane (azimuth =  $0.5^\circ$ ) along north. The antenna size is  $23.8 \lambda$ , and a peak sidelobe level of  $-24$  dB is measured. Variables of the template plotted in Fig. 3 are  $\psi_0 =$

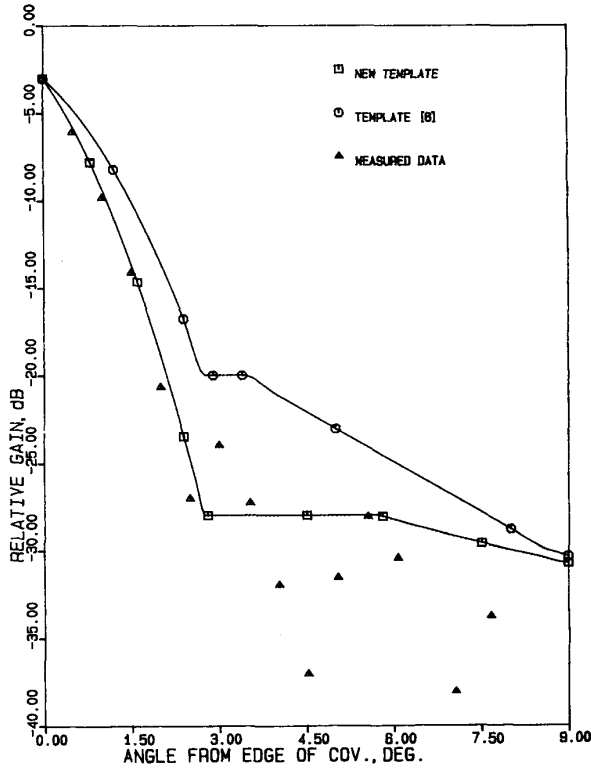


Fig. 3. Comparison of new template with Brazilsat measured data in elevation plane (azimuth =  $0.5^\circ$ ) along north (frequency = 3.96 GHz,  $D/\lambda = 23.8$ ). Parameters of template are  $S = 0.5023$  and  $\psi_0 = 6.0^\circ$ .

$6^\circ$  and  $S = 0.5023$ . A reasonable agreement is noticed between the template and the Brazilsat measurement except in the angular region close to the first sidelobe peak. No sidelobe suppression techniques have been employed in the design. The IWP 4/1 template shown in Fig. 3 is again conservative in comparison to the measured data and the new template. The new template when compared with the earlier one [1] is four percent broader for Anik-E (with a maximum scan of 4 beamwidths) and three-percent narrower for Brasilsat (having a maximum scan of 1 beamwidth) in the main lobe skirt region. Further, the new template has been found to compare well the measured data on other satellite antennas. Details of the comparison results on Anik-C, G-Star, TDRSS, INTELSAT V, etc., can be found in [2].

#### IV. CONCLUSION

A new template is developed for shaped-beam satellite antennas by taking into consideration the primary as well as the secondary parameters. The variables of the template are the coverage region width ( $\psi_0$ ) in the direction of interest and the shaping factor  $S$ . The template is found to be a reasonable upper bound specification for future satellite antennas. Low sidelobe levels as well as steeper main beam gain fall-off rate could be achieved for future satellites by using larger antenna aperture and more component beams.

#### APPENDIX

The effects of the secondary parameters on the satellite antenna radiation outside the coverage area are quantified here by using simple approximate equations. Main beam broadening and increase in the sidelobe levels due to the three secondary parameters are

expressed as

$$\theta_0(s, \Delta, \delta) = \theta_0 \cdot \exp(0.5s^2) \cdot [\eta_i(\Delta)]^{-0.5} 10^{\{0.000075\delta^2 / [(F/D_p)^2 + 0.02]^2\}} \quad (12)$$

and

$$S_L(s, \Delta, \delta) = S_L + (3.26s^2 + 2.57s) + 10 \log [(1 + 0.32\sqrt{\Delta}\nu)^2 / \eta_i(\Delta)] + (1.3x - 0.016x^2) \quad (13)$$

where  $s = 4\pi(\epsilon/\lambda)$  is the rms surface deviation,  $\Delta$  is the blockage parameters (square root of the ratio between the area blocked and the aperture area),  $\delta$  is the number of beamwidths scanned away from the boresight, and  $\theta_0$  is the 3-dB beamwidth of the antenna without the secondary effects.  $\eta_i$  and  $x$  in (12) and (13) are given as

$$\eta_i(\Delta) = (1 - \Delta^2)^2, \quad \text{for central blockage} \\ = [1 - \{1 - A(1 - \Delta^2)\} \Delta^2]^2, \quad \text{for edge blockage} \quad (14)$$

$$x = \delta / [(F/D_p)^2 + 0.02]. \quad (15)$$

The variable  $A$  in (14) is the pedestal height in the illumination function ( $1 - Ar^2$ ),  $\nu$  is the ratio of the field amplitude at the center of blocked area to the field amplitude at the aperture edge,  $F$  is the focal length, and  $D_p$  is the diameter of the parent paraboloid. In (12) and (13), the surface error effects are derived based on Ruze's statistical approach [8], [9]; aperture blockage is accounted for using the geometrical optics method (diffraction effects are neglected) [10], [11], and the scan effects are derived by interpolating the results given in [12]. The formulas are valid for secondary parameters in the range  $0 \leq s \leq 0.3$ ,  $0 \leq \Delta \leq 0.15$ , and  $0 \leq x \leq 50$  (which corresponds to a maximum of nine beamwidths scan for  $F/D_p = 0.4$ ). Further details of the derivations of (12) and (13) are given in [2].

#### ACKNOWLEDGMENT

The author would like to thank Mr. V. Sahay of the Department of Communications, Ottawa, for many useful discussions and encouragement. Contributions and suggestions from colleagues Dr. H. J. Moody, Dr. C. C. Huang, Mr. A. Baylis, and Mr. D. Nguyen are gratefully acknowledged. The author is indebted to the anonymous reviewers for their critical review and useful suggestions.

#### REFERENCES

- [1] K. S. Rao and H. J. Moody, "Modeling of shaped beam satellite antenna patterns," *IEEE Trans. Antennas Propagat.*, vol. AP-35, pp. 632-642, June 1987.
- [2] K. S. Rao, A. Baylis, and H. J. Moody, "Recommendation of a template for shaped beam satellite antenna patterns," Spar Aerospace Limited, Ste Anne de Bellevue, Quebec, PQ, Canada, Rep. RML-009-87-081, June 1987.
- [3] D. F. DiFonzo, "The evolution of communications satellite antennas," in *IEEE APS Symp. Dig.*, Albuquerque, NM, May 1982, pp. 358-361.
- [4] CCIR Rep. 558-2 (MOD 1), "Satellite antenna patterns in the fixed satellite service," Study Program 2J/4, 1984.
- [5] CCIR Study Group, "Revision to Report 558-2: Spacecraft shaped beam antenna pattern," Doc. 4/253-E, June 25, 1985.
- [6] 14th Rep. CCIR Working Party 4/1, "Satellite reference patterns," DOC.4/1 (Rev. 1), Rio de Janeiro, Brasil, May 1987, pp. 121-152.
- [7] "Revision of the FSS satellite antenna reference pattern," ERA Technologies Ltd, Report, England, Mar. 1987.
- [8] J. Ruze, "Antenna tolerance theory—A review," *Proc. IEEE*, vol. 54, pp. 633-640, Apr. 1966.
- [9] A. W. Rudge, et al., *The Handbook of Antenna Design*, vols. 1 and 2. England: Peregrinus, 1986, p. 134.
- [10] K. S. Rao and P. S. Kildal, "A study of the diffraction and blockage

- effects on the efficiency of the Cassegrain antennas," *Canadian Elec. Eng. J.*, vol. 9, pp. 10-15, Jan. 1984.
- [11] C. Dragone and D. C. Hogg, "The radiation pattern and impedance of offset and symmetrical near-field Cassegrain and Gregorian antennas," *IEEE Trans. Antennas Propagat.*, vol. AP-22, pp. 472-475, May 1974.
- [12] J. Ruze, "Lateral-feed displacement in a paraboloid," *IEEE Trans. Antenna Propagat.*, vol. 13, pp. 660-665, Sept. 1965.

### Realizable Feed-Element Patterns and Optimum Aperture Efficiency in Multibeam Antenna Systems

K. S. YNGVESSON, MEMBER, IEEE, J. F. JOHANSSON, STUDENT MEMBER, IEEE, Y. RAHMAT-SAMII, FELLOW, IEEE, AND Y. S. KIM, STUDENT MEMBER, IEEE

**Abstract**—The results of an earlier paper by Rahmat-Samii *et al.*, regarding realizable patterns from feed elements which are part of an array which feeds a reflector antenna, are extended. The earlier paper used a  $\cos^q \theta$  model for the element radiation pattern, while here we perform a parametric study, employing a model which assumes a central beam of  $\cos^q \theta$  shape, with a constant sidelobe level outside the central beam. Realizable  $q$ -values are constrained by the maximum directivity based on feed element area. The optimum aperture efficiency [excluding array feed network losses] in an array-reflector system is also evaluated as a function of element spacing using this model, as well as the model of the earlier paper. Experimental data for tapered slot antenna (TSA) arrays are in agreement with the conclusions based on the model.

#### INTRODUCTION

Multibeam antenna systems, using either a reflector or a lens as the focusing element [1]-[3], continue to be of considerable interest for a number of applications. Such systems typically employ a periodic two-dimensional array of feed elements, to be able to project a number of beams to different directions with each beam being radiated by one or more of the individual feeds in the array. The arrays may differ somewhat in terms of the phasing of the feed elements depending on the intended application. Satellite communication antennas, for example, may use a prescribed number of feeds as a subarray with specific amplitude- and phase relationships to shape a beam [4]. Other systems, such as those used for millimeter-wave imaging [5], detect the signal picked up by each feed independently.

An important parameter to consider when one designs multibeam systems is the crossover level, i.e., the level below the peak of each beam at which it crosses the neighboring beam. The crossover level can be raised by placing the feed elements at as small a spacing as possible. Multibeam imaging systems may instead be characterized in

Manuscript received December 24, 1986; revised October 10, 1987. This work was supported in part by the Nasa Langley Research Center under Contract NAS-1-18310.

K. S. Yngvesson and Y. S. Kim are with the Department of Electrical and Computer Engineering, University of Massachusetts, Amherst, MA 01003.

J. F. Johansson was with the Department of Electrical and Computer Engineering, University of Massachusetts, Amherst, MA. He is now with the Department of Radio and Space Science, Chalmers University of Technology, Gothenburg, Sweden.

Y. Rahmat-Samii is with the Jet Propulsion Laboratory, California Institute of Technology, Pasadena, CA 91109.

IEEE Log Number 8823414.

terms of how closely the angular resolution (i.e., the angular distance between beams) approaches the sampling-limited resolution. For clarity, we will emphasize the use of crossover level in this communication, although the approach to be presented can easily be adapted for the evaluation of imaging systems with focal-plane arrays as well.

One typically assumes that the feed elements completely fill the aperture of the array, and thus the area of each element must be decreased as the spacing is decreased. Smaller area elements have lower directivity, and larger spillover losses will inevitably result from an attempt to raise the crossover level in this manner. One is led to investigate feed elements which have the narrowest possible beam for a given spacing (i.e., a given area), and an investigation of this kind was carried out by Rahmat-Samii *et al.* [3]. This paper used a  $\cos^q \theta$  model for the radiation patterns of the elements.

Here we extend the results of [3] to take into account a class of feed elements with a prescribed sidelobe structure outside a  $\cos^q \theta$  central beam. We also show explicitly the limitations on the aperture efficiency which can be attained for multibeam systems, using arrays with varying feed element spacings, and for different classes of such elements. The aperture efficiency calculation shows the trade-offs involved between aperture efficiency and crossover level as the element spacing is used to change the latter. The similar trade-off between spillover efficiency and taper efficiency for a single-beam reflector antenna which occurs as the beamwidth of the feed (or equivalently its aperture area) is varied is very well known [6]. In calculating the aperture efficiency in multibeam systems, we must impose a constraint on the maximum element directivity for a given element area, a constraint which does not appear in the single-beam case. Explicit calculations of this type do not appear to have been published previously.

#### ANALYSIS USING $q$ -VALUE BASED ON DIRECTIVITY

As in [3], we will approximate the radiation pattern of a typical ideal feed near its main beam region by a cosine function:

$$E(r) \sim \frac{e^{-jkr}}{4\pi r} [\hat{\theta}U_1 - \hat{\phi}U_2], \quad r \rightarrow \infty \quad (1a)$$

where

$$U_1 = (\cos \theta)^{q_1} \cos \phi \quad U_2 = (\cos \theta)^{q_2} \sin \phi. \quad (1b)$$

We also assume for simplicity that the radiation patterns in the  $E$ - and  $H$ -planes are identical. As shown in [3], the feed directivity  $D$  is given by

$$D = 2(2q + 1). \quad (2)$$

Also, for the feeds considered in [3],  $q$  is a quadratic function of  $d/\lambda$ , i.e.,

$$q = \kappa(d/\lambda)^2 - 0.5. \quad (3)$$

It is of interest to investigate the maximum possible value of  $q$  for any feed ( $q_{\max}$ ) at a given spacing  $d/\lambda$  which is found by using the maximum value for the directivity:

$$D_{\max} = 4\pi A_{el}/\lambda^2. \quad (4)$$

Equation (4) gives the maximum directivity for an element in a large array (i.e., essentially infinite in the sense that edge effects can be neglected) based on the element area  $A_{el}$  [7], [8]. The element area